RESEARCH ARTICLE

OPEN ACCESS

Analysis of Fault Lines in the City of Manado

Fabian J Manoppo[1,*], Lianly Hendrata[1] and Yudi O Waany[2]

[1]Department of Civil Engineering, Faculty of Engineering, Sam Ratulangi University, Indonesia
[2]Department of Architecture, Faculty of Engineering, Sam Ratulangi University, Indonesia

Abstract:

Background: The Indonesian region with high seismic activity, Manado City, is situated at the convergence of four major tectonic plates on Earth: the Eurasian Plate, Indo-Australian Plate, Pacific Plate, and Philippine Plate.

Aim: This study aimed to identify the Manado fault line. The Geoelectric PQWT-TC 300 tool was utilized, which could detect up to a depth of 300 meters vertically.

Objective: The research wasconducted to analyze and to create a map of the Manado fault line. This studyis one of the efforts to mitigate earthquake disasters, which involves constructing earthquake-resistant infrastructure.

Methods: The Manado fault line was measured for 17 lines; each line was 9 to 41m in length, and the result was found to be Manado fault at line 23 Kayuragi-1 and line 70 among the 17 lines.

Results: The depth of the Manado Fault started from 30m to 270m from the surface layer. The resistivity values of fault were 0 Ω.

Conclusion: The present identification of the Manado fault line was close to the previous analysis, and the activity of the Manado fault line has not been detected in the last 1800 years. The present method yielded a better result for the Manado fault line than the previous method.

Keywords: Manado fault line, Geoelectric PQWT, Manado city.

*Address correspondence to this author at the Department of Civil Engineering, Faculty of Engineering, Sam Ratulangi University, Indonesia; E-mail: fabian_jm@yahoo.com

1. INTRODUCTION

Sulawesi is a region located at the convergence of major tectonic plates, namely the Pacific Plate, Eurasian Plate, Indo-Australian Plate, and the smaller Philippine Plate. These plates move in a convergent manner, resulting in several faults running through the North Sulawesi region. The seismic condition of North Sulawesi [1-8] shows that the province of North Sulawesi is located near the following subduction zones: the North Sulawesi Trench/Minahasa Trench and the Sangihe Double Subduction/East and West Molucca Sea. Additionally, there are several active fault lines within a relatively close radius of this province. These fault lines include the Gorontalo North and South, Tomini, Batui Thrust, and Balantak faults. There are also the Tondano, Amurang, Kotamobagu, and Manado faults, which are active, but their characteristics are not yet known. Earthquakes in Manado City occurred onshore, as predicted by the Manado Fault from 1800 until 2023, based on USGS website data, which are shown in Fig. (**1**).
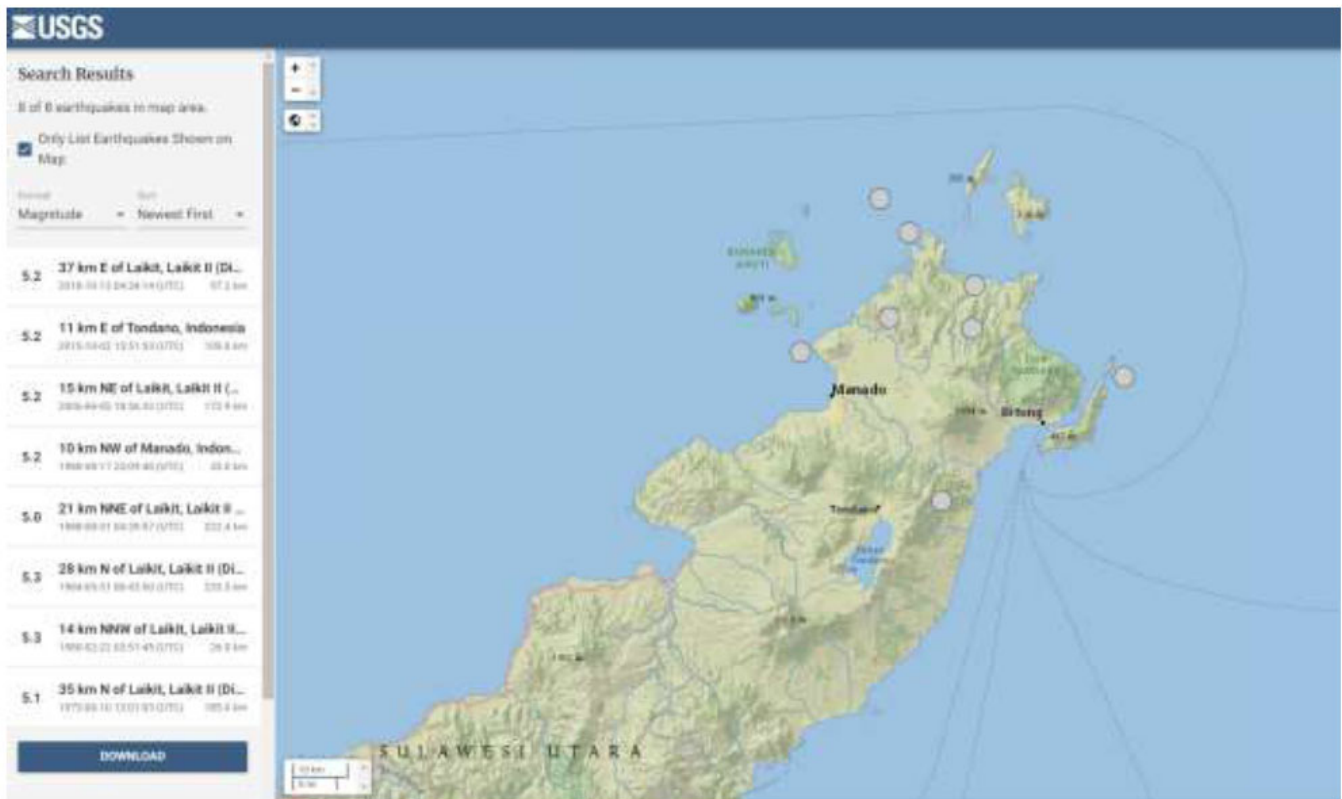
Fig. (1). Earthquake map of manado fault.

Fig. (2). Geology map of manado fault.

These conditions contribute to the high risk of earthquakes in this province, as evidenced by the frequent earthquakes occurring in and around the region, which can be felt in densely populated areas. Manado City is one of the areas in North Sulawesi with the highest population density compared to other cities in the province. The high population density, the presence of vital infrastructure, such as hospitals and schools, and the existence of several tall buildings in Manado City make it susceptible to significant casualties, infrastructure damage, and losses in the event of an earthquake. Given the high seismicity and risk, any infrastructure development in this area must consider and account for the local seismic conditions. Additionally, with various other disaster analyses, mitigation measures can be implemented. One of the mitigation efforts that can be undertaken is to identify the Manado fault line and conduct further analysis of its level of activity, depth, and direction. Further, a method to analyze fault lines has been put forward [9-17]. By understanding the Manado fault line, which is connected to the Palu Koro fault, mitigation measures can be taken to minimize the impact of earthquakes caused by this fault, as shown in Fig. (**2**).

This research was done conducted about 17 lines, and the location of the research is shown in Fig. (**3**).

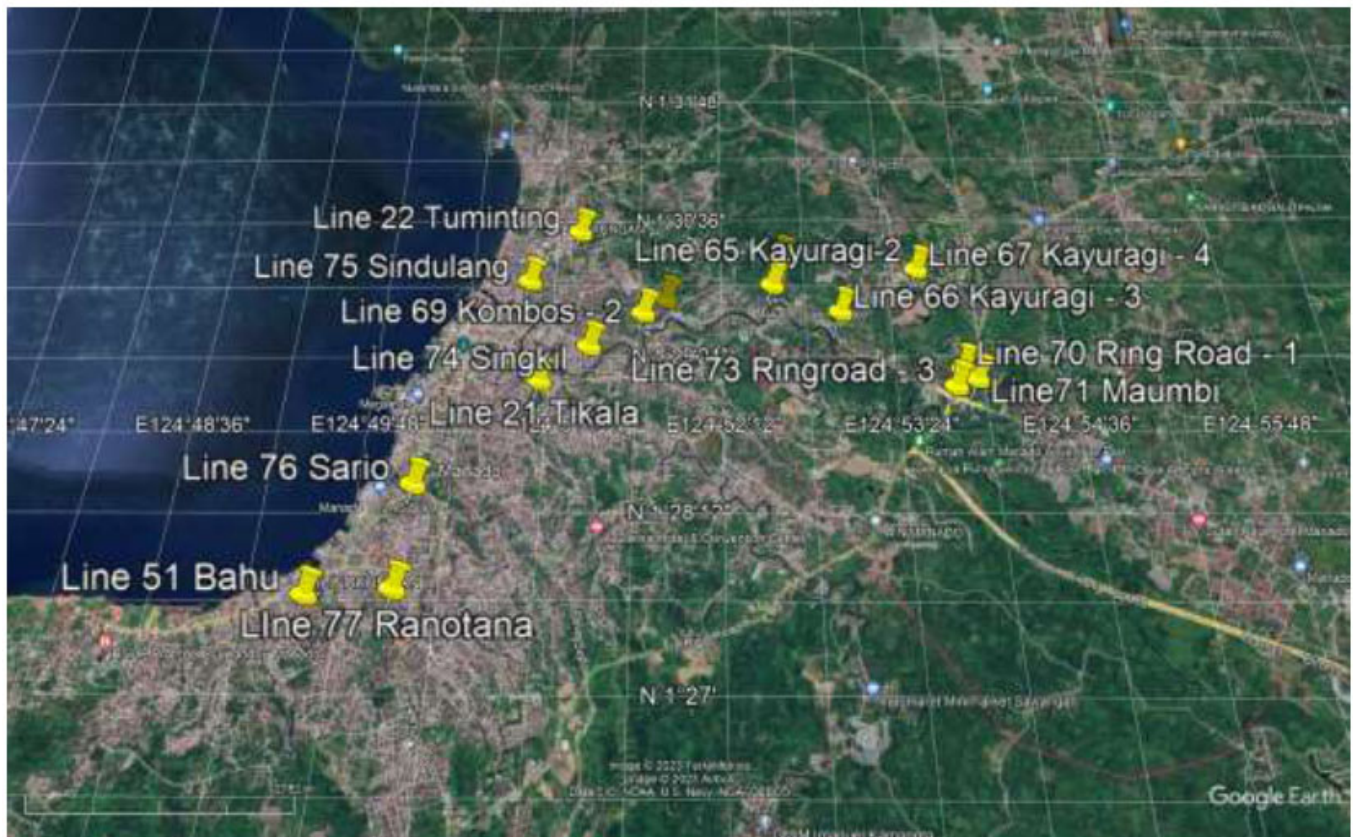The coordinates of the fault analysis of Manado City are shown in Table **1**.

Fig. (3). The number of location research.

Table 1. Coordinate fault analysis of Manado city.

Number	Line Number	Coordinate	Length of Measurement (m)	Name of Place
1	21	1°29'2.21"N 124°50'54.02"E	11	Tikala Manado City
2	22	1°30'18.82"N 124°51'7.71"E	15	Tuminting Manado City
3	23	1°30'3.72" N 124°52'34.92" E	15	Kairagi – 1 Manado City

(Table 1) contd.....

Number	Line Number	Coordinate	Length of Measurement (m)	Name of Place
4	51	1°27'28.79"N 124°49'32.80"E	9	Bahu Manado City
5	65	1°29'50.52"N 124°52'31.30"E	36	Kairagi – 2 Manado City
6	66	1°29'36.67"N 124°52'59.84"E	21	Kairagi – 3 Manado City
7	67	1°29'57.65"N 124°53'33.38"E	21	Kairagi – 4 Manado City
8	68	1°29'42.63"N 124°51'45.66"E	26	Kombos -1 Manado City
9	69	1°29'35.22"N 124°51'36.22"E	34	Kombos -2 Manado City
10	70	1°29'8.06"N 124°53'48.56"E	21	Ring Road – 1 Manado City
11	71	1°29'3.13"N 124°53'53.71"E	21	Maumbi North Minahasa
12	72	1°29'8.86"N 124°53'49.57"E	31	Ring Road – 2 Manado City
13	73	1°28'59.81"N 124°53'44.98"E	33	Ring Road – 3 Manado City
14	74	1°29'18.98"N 124°51'13.86"E	41	Singkil Manado City
15	75	1°29'51.91"N 124°50'47.16"E	21	Sindulang Manado City
16	76	1°28'14.57"N 124°50'7.91"E	21	Sario Manado City
17	77	1°27'31.23"N 124°50'5.32"E	16	Ranotana Manado City

2. METHOD

To analyse fault lines, various instruments and methods can be used, such as Seismic Reflection and Refraction, Ground Penetrating Radar (GPR), Electrical Resistivity Tomography (ERT), Light Detection and Ranging (LIDAR), Paleoseismology, Satellite Imagery and Remote Sensing, and Interferometric Synthetic Aperture Radar (GPS and InSAR). Among these methods, the Geoelectric PQWT TC-300 offers advantages, such as portability, ease of deployment in various field conditions, real-time data providing immediate feedback on subsurface anomalies, and being non-invasive, thus not requiring extensive drilling or excavation. Some methods are available according to the guidebook on the use of geoelectric PQWT TC-300 devices, as shown in Fig. (**4**). The apparatus operates with a new methodology that differs from the old geoelectric tool. The methodology developed in geophysical exploration is a newly developed working principle known as the Natural Electric Field Frequency Selection System for geophysical instruments, commonly referred to as the frequency system. The instrument works based on the principle of the natural electric field magnetic field difference of the Earth (frequency range of 0-30 kHz). Several changes in the frequency of electromagnetic fields are used to study changes in the underground field/material to solve geological problems. It is one of the methods for alternating current exploration. By utilizing the natural electric field source as the working area, the contrasting resistivity of rocks, underground minerals, and groundwater can be studied. The natural electric field

components are measured on the surface with different frequency fields, allowing for the study of variations in geological areas and solving geological problems. This is a method of electrical prospecting. Since this method measures the electrical component of the electromagnetic field of the Earth, it is called the natural electric field method. The appropriate frequency is selected for measurements within -50 meters, and the selected frequency is known as the frequency selection method or the natural potential frequency method. According to this theory, the design and production of equipment known as potential frequency detection instruments refer to instruments that measure the natural electric field frequency or instruments used for geological exploration work. Therefore, from a professional point of view, geological equipment should be classified as part of geophysical equipment among electrical instruments. This device can detect fault lines, water, caves in the ground, geothermal activity, archaeology, logging tools, *etc*, by using the resistivity value and colour type, as shown in Figs. (**5** and **6**). From the perspective of measuring field source classification, it is also known as a natural electric field instrument, audio electric field instrument, or audio earth instrument. The instrument uses natural earth field sources without artificial fields and eliminates the clumsy power supply system to achieve a simple and lightweight instrument. After collecting data with its unique built-in computational function, the instrument can automatically plot curve graphs and profile maps with a single button press, allowing for a clear understanding of the geological structure and quick determination of rock formations, fault lines, underground caves, aquifers, *etc*.
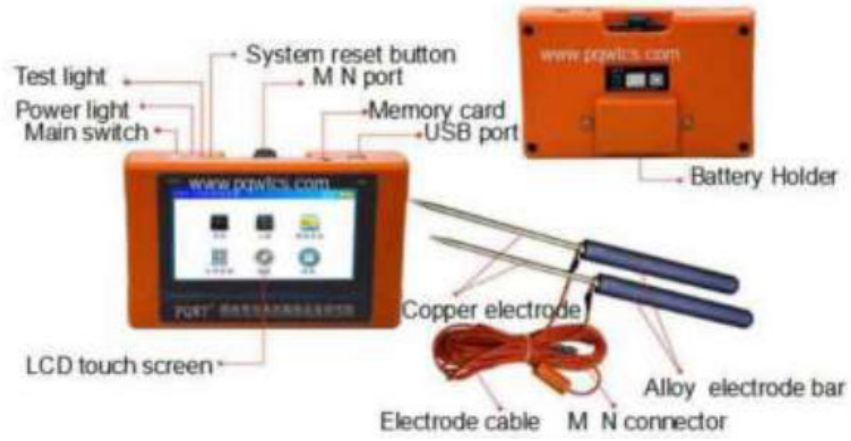
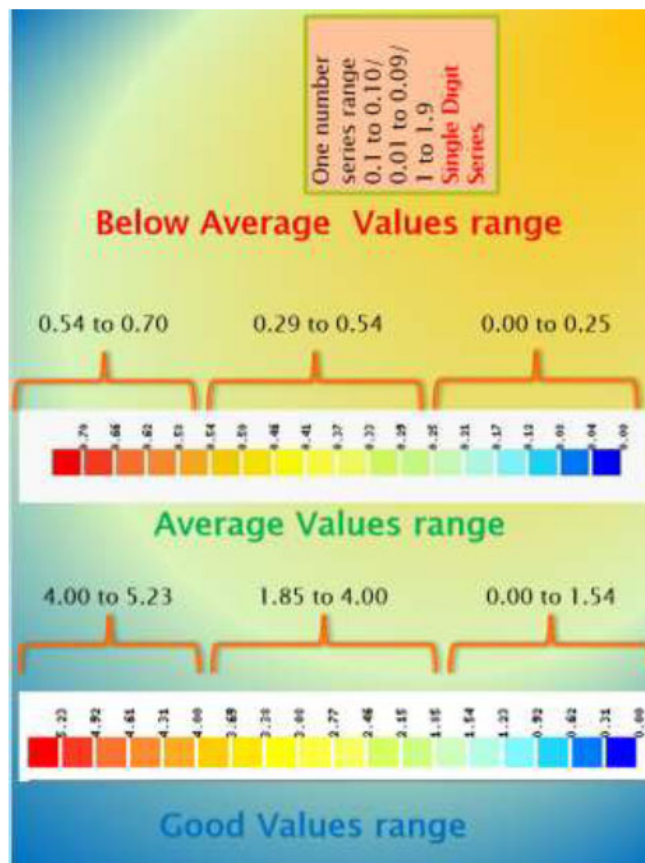- **PQWT-TC300**

Fig. (4). PQWT-TC300 instrument.

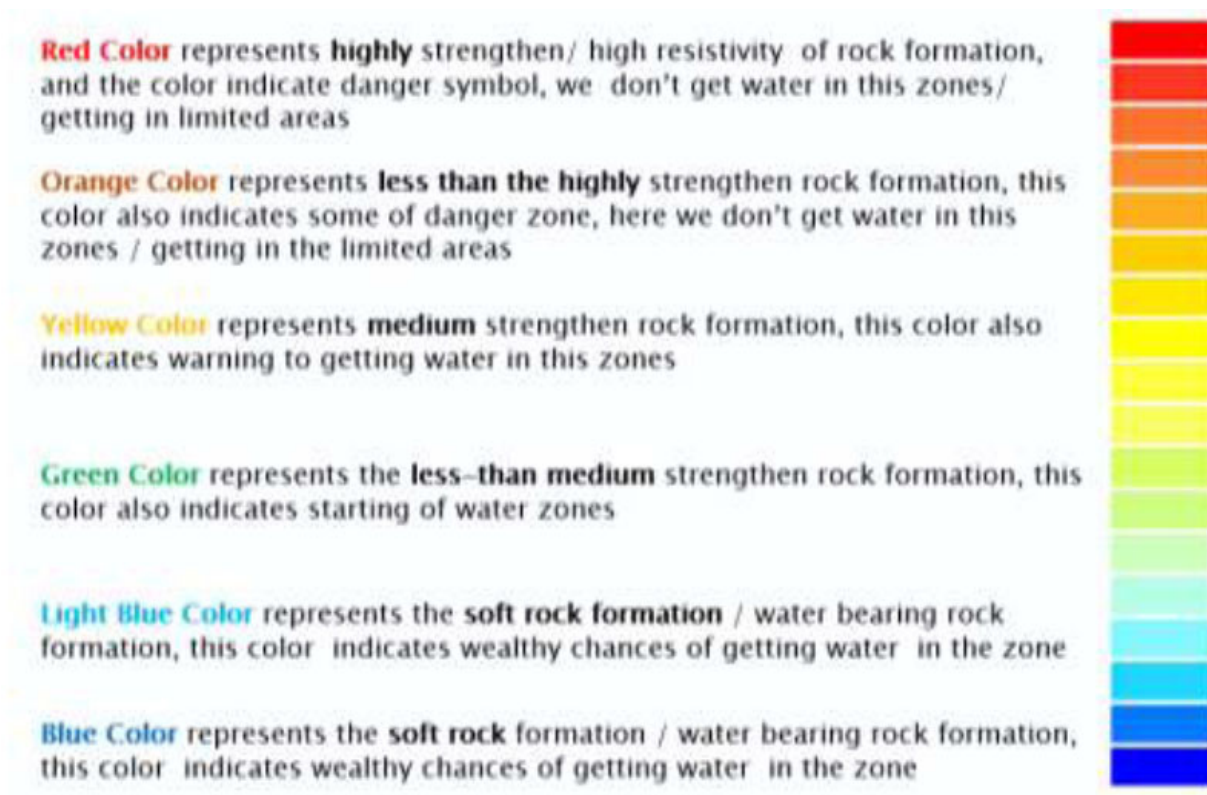**Fig. (5).** Resistivity value represented the color.

Red Color represents **highly** strengthen/ high resistivity of rock formation, and the color indicate danger symbol, we don't get water in this zones/ getting in limited areas

Orange Color represents **less than the highly** strengthen rock formation, this color also indicates some of danger zone, here we don't get water in this zones / getting in the limited areas

Yellow Color represents **medium** strengthen rock formation, this color also indicates warning to getting water in this zones

Green Color represents the **less–than medium** strengthen rock formation, this color also indicates starting of water zones

Light Blue Color represents the **soft rock formation** / water bearing rock formation, this color indicates wealthy chances of getting water in the zone

Blue Color represents the **soft rock** formation / water bearing rock formation, this color indicates wealthy chances of getting water in the zone

Fig. (6). Resistivity value represented the color.

Table 2. Results analysis of manado fault line.

Line	Located	Strength	Water Potential	Fault
21	Tikala Manado	Weak Zone	High	No
22	Tuminting, Manado	Weak Zone	High	No
23	Kairagi-1, Manado	Weak Zone	High	Depth of 120-270 m
51	Bahu, Manado	Strong Zone	No	No
66	Kairagi-3, Manado	Strong Zone	No	No
67	Kairagi-4, Manado	Strong Zone	No	No
68	Kombos-1, Manado	Strong Zone	No	No
69	Kombos-2, Manado	Strong Zone	No	No
70	Ring Road-1, Manado	Weak Zone	High	Dept of 30-270 m
71	Maumbi, North Minahasa	Strong Zone	No	No
72	Ring Road-2, Manado	Strong Zone	No	No
73	Ring Road-3, Manado	Strong Zone	No	No
74	Singkil, Manado	Strong Zone	No	No
75	Sindulang, Manado	Strong Zone	No	No
76	Sario, Manado	Strong Zone	No	No
77	Ranotana, Manado	Strong Zone	No	No

3. RESULTS & DISCUSSION

The Manado fault line was measured for 17 lines; each line was 9 to 41m in length, and the result was found as shown in Table **2**, Figs. (**7-23**).

Line 21 at Tikala, Manado city, at the coordinates 1°29'2.21"N, 124°50'54.02"E, showed a weak zone area with high water potential from 0 to 90m. There was no fault indicated, as shown in Fig. (**7**).
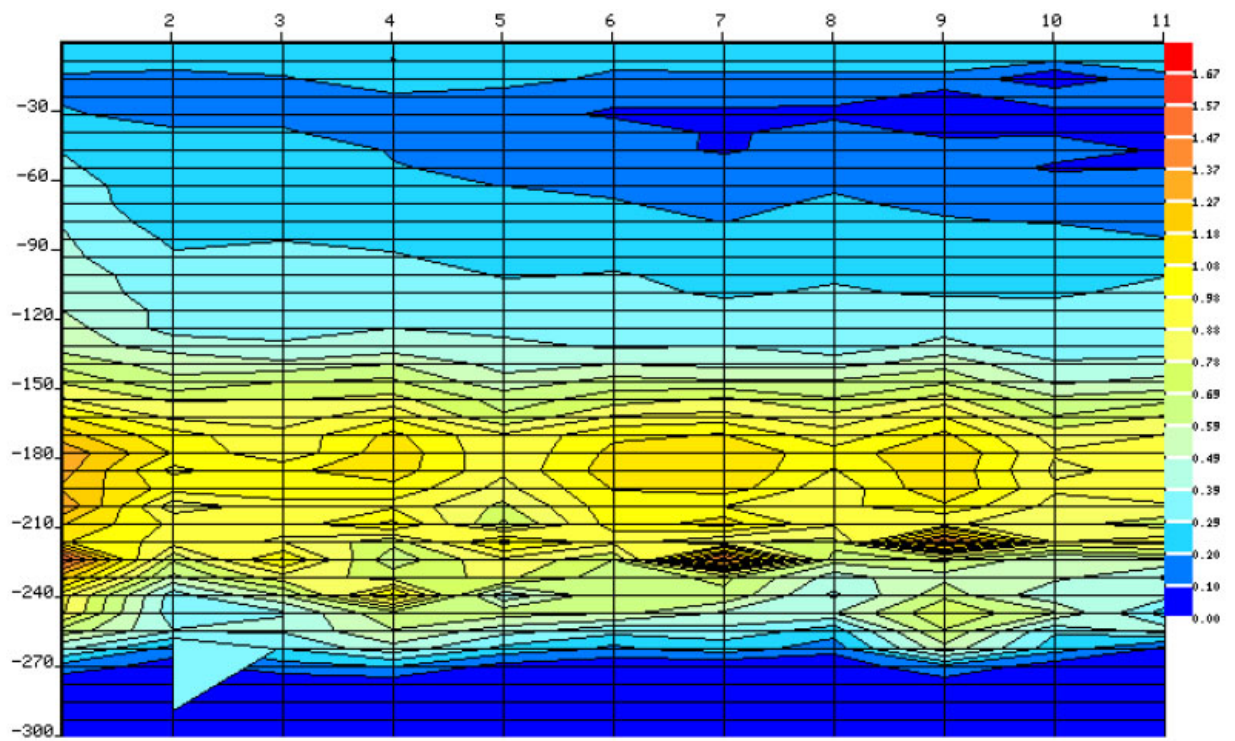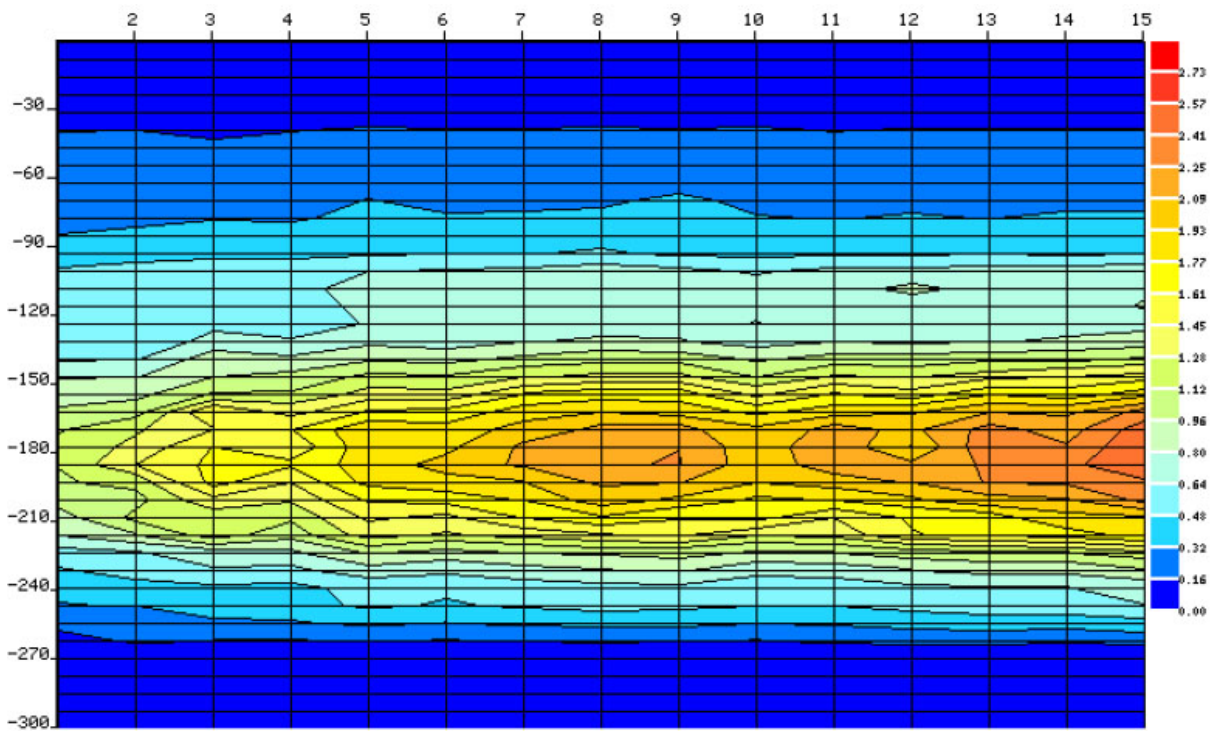
Fig. (7). Line 21 tikala Manado city.

Fig. (8). Line 22 tuminting Manado city.

Line 22 at Tuminting, Manado city, at the coordinates 1°30'18.82"N, 124°51'7.71"E, showed a weak zone area with high water potential from 0m to 90m. There was no fault indicated, as shown in Fig. (**8**).

Line 23 Kairagi-1, Manado city, at the coordinates 1°30'3.72" N, 124°52'34.92" E, showed a weak zone area with high water potential from 0 to 120m. There was found fault from a depth of 120m to 270m, as shown in Fig. (**9**).
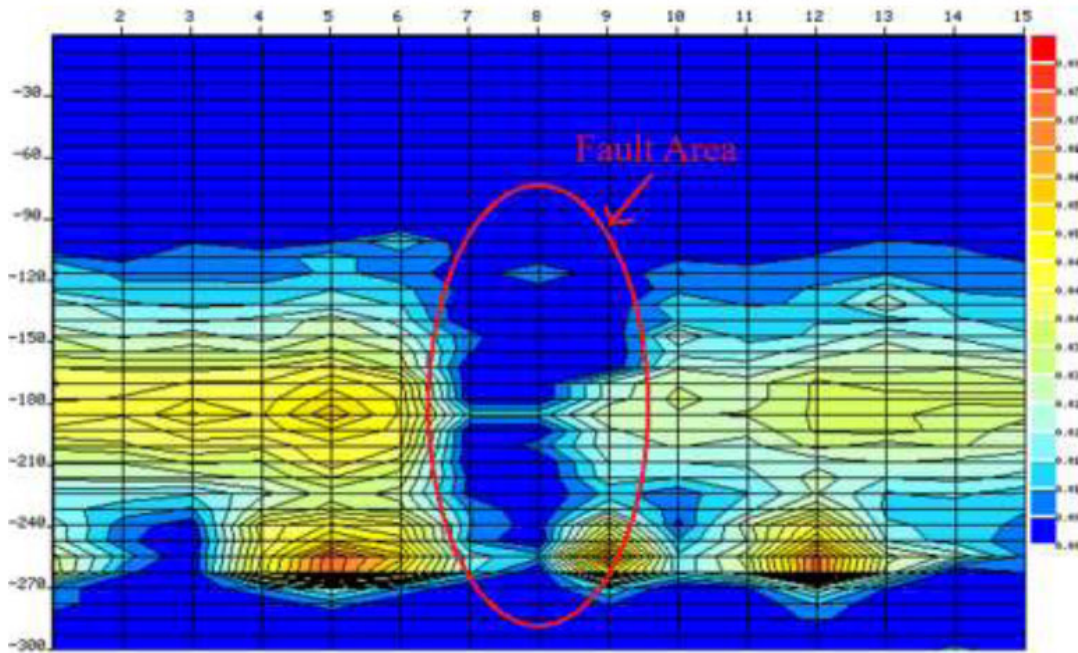
Fig. (9). Line 23 kairagi – 1 Manado city.
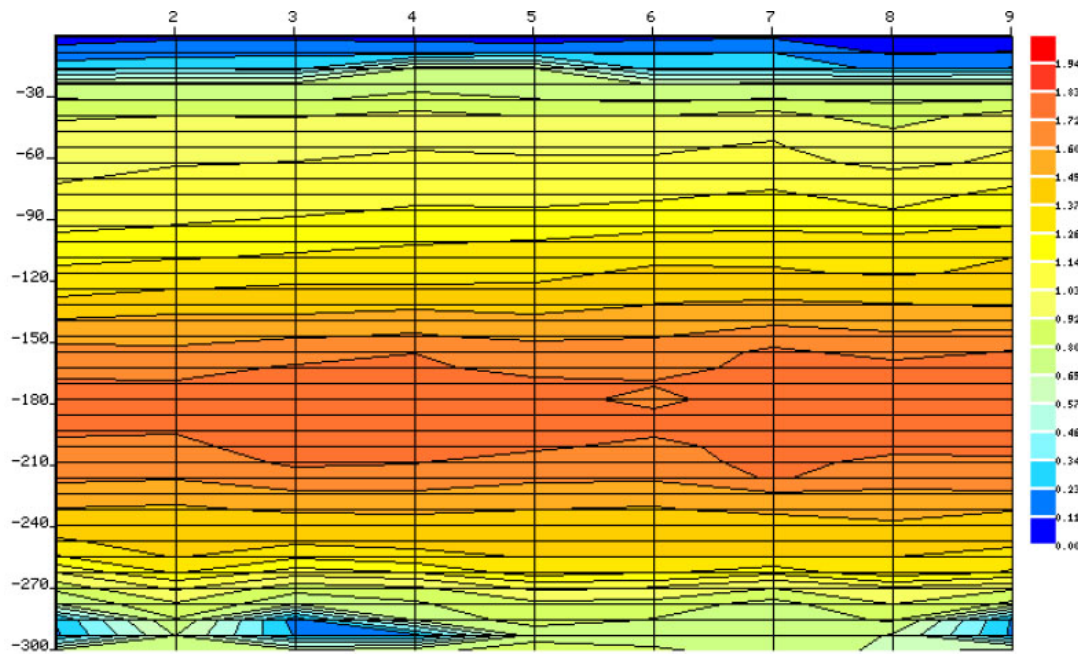
Fig. (10). Line 51, Bahu Manado city.

Line 51 Bahu, Manado city, at the coordinates 1°27'28.79"N, 124°49'32.80"E, showed a strong zone area with no water potential. There was no fault, as shown in Fig. (**10**).

Line 65 Kairagi-2 Manado city, at the coordinates 1°29'50.52"N, 124°52'31.30"E, showed a strong area with no water potential. There was no fault, as shown in Fig. (**11**).
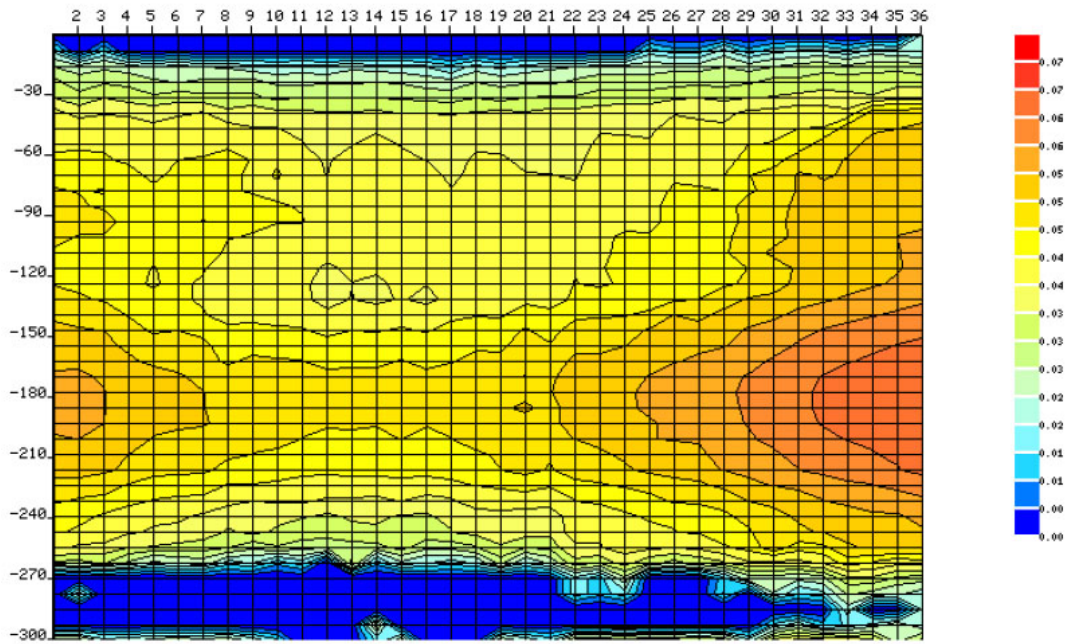
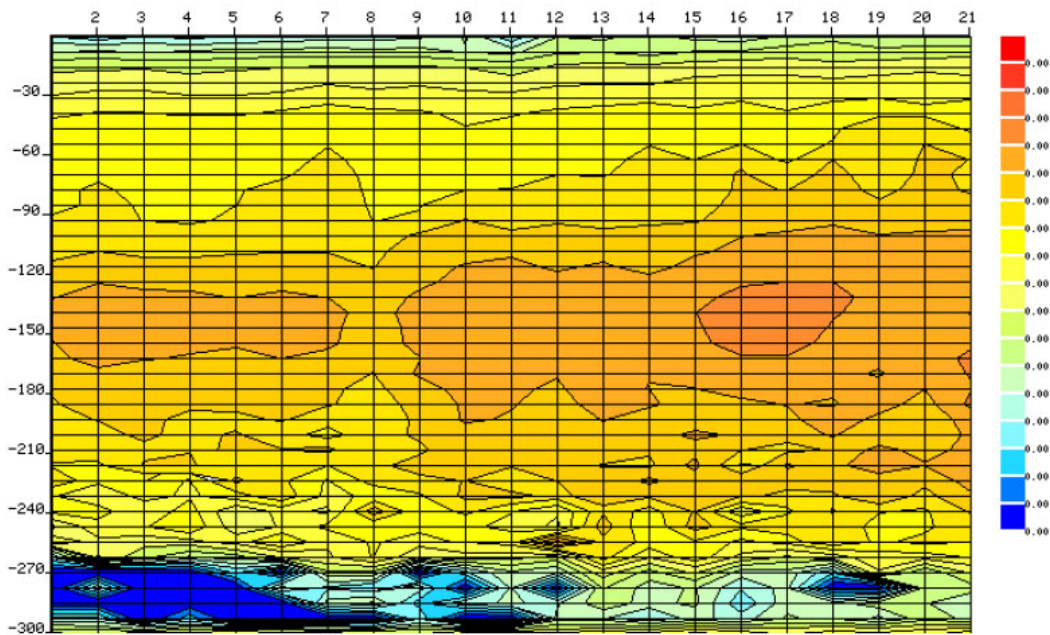**Fig. (11).** Line 65 Kairagi -2 Manado City

Fig. (12). Line 66 Kairagi – 3 Manado city.

Line 66 Kairagi-3, Manado city at the coordinates 1°29'36.67"N, 124°52'59.84"E showed a strong zone area with no water potential. There was no fault, as shown in Fig. (**12**).

Line 67 Kairagi-4, Manado city, at the coordinates 1°29'57.65"N, 124°53'33.38"E, showed a strong zone area with no water potential. There was no fault, as shown in Fig. (**13**).

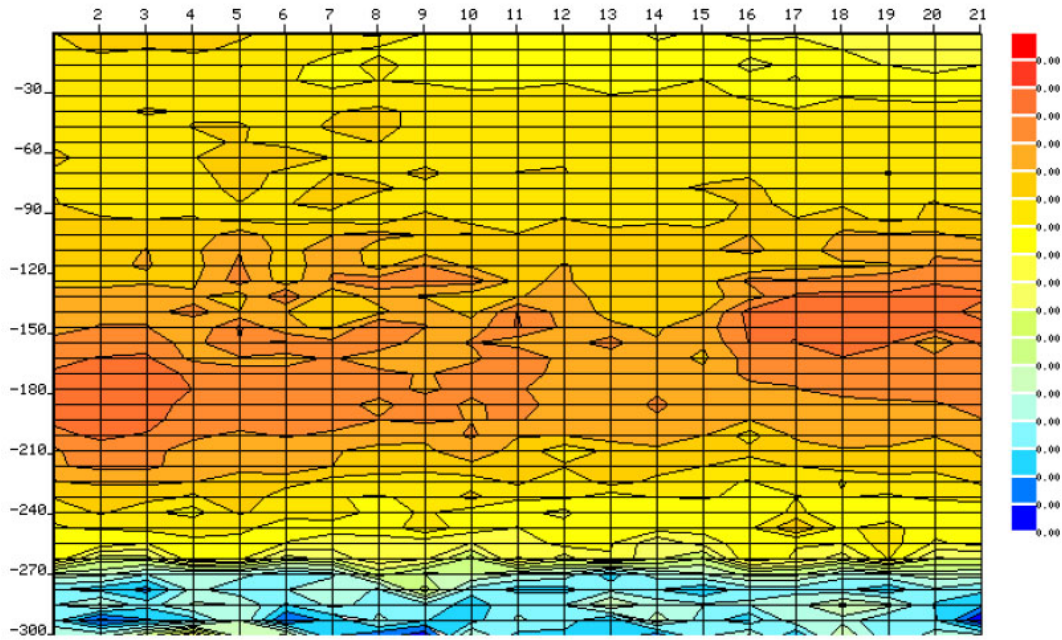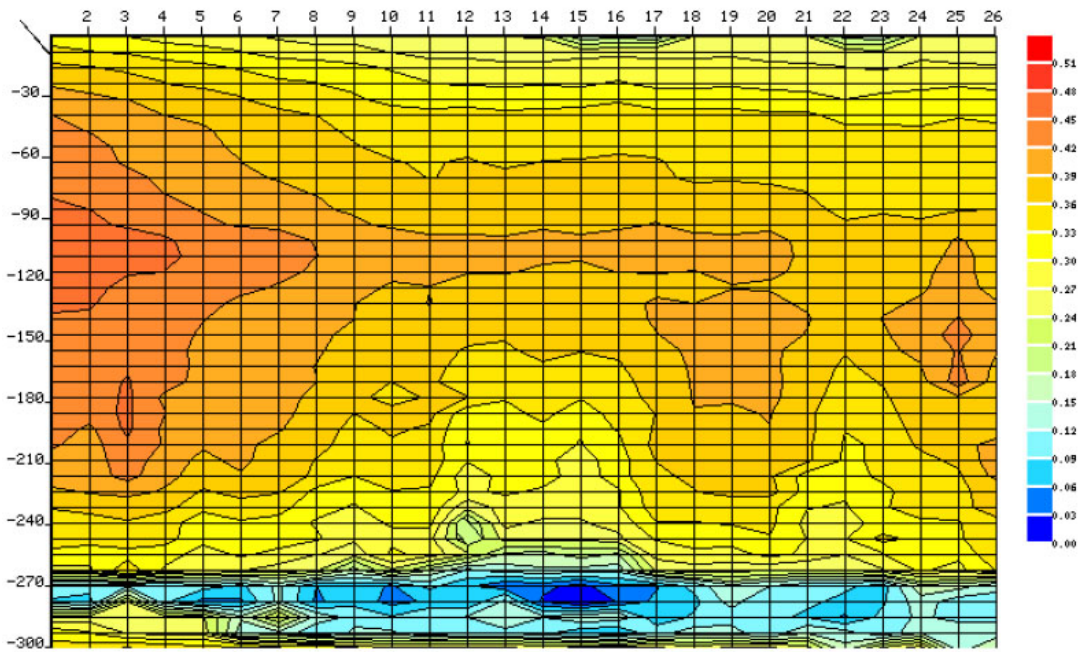**Fig. (13).** Line 67 Kayuragi – 4 Manado city.

Fig. (14). Line 68 Kombos – 1 Manado city.

Line 68 Kombos – 1, Manado city, at the coordinates 1°29'42.63"N, 124°51'45.66"E, showed a strong zone area with no water potential. There was no fault, as shown in Fig. (**14**).

Line 69 Kombos – 2, Manado city, at the coordinates 1°29'35.22"N, 124°51'36.22"E, showed a strong zone area with no water potential. There was no fault, as shown in Fig. (**15**).
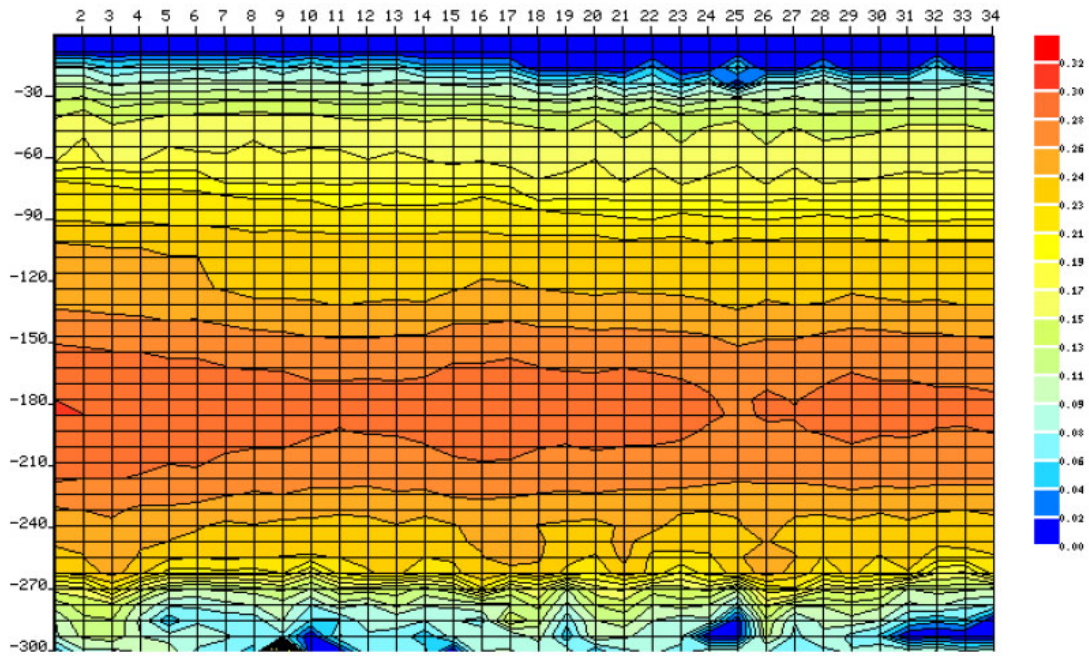

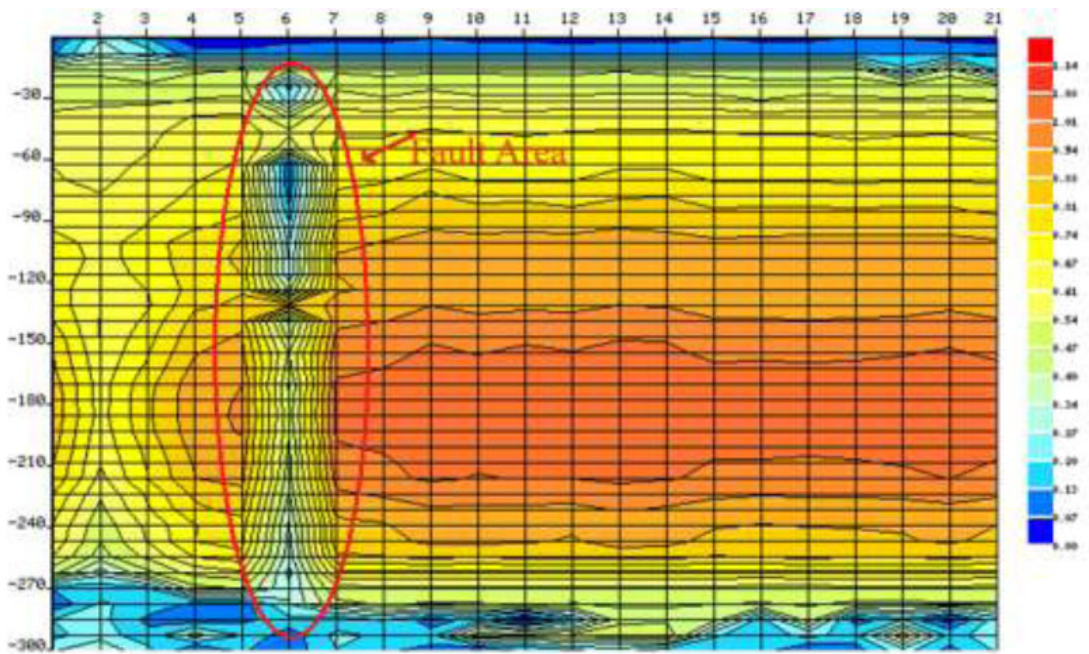**Fig. (15).** Line 69 Kombos – 2 Manado city.

Fig. (16). Line 70 Ring Road – 1 Manado city.

Line 70 Ring Road – 1, Manado city, at the coordinate 1°29'8.06"N, 124°53'48.56"E, showed a weak zone area with high water potential. A fault was found at a depth of 30m to 270m, as shown in Fig. (**16**).

Line 71 Maumbi, Minahasa Utara, at the coordinate 1°29'3.13"N, 124°53'53.71"E, showed a strong zone area with no water potential. There was no fault, as shown in Fig. (**17**).
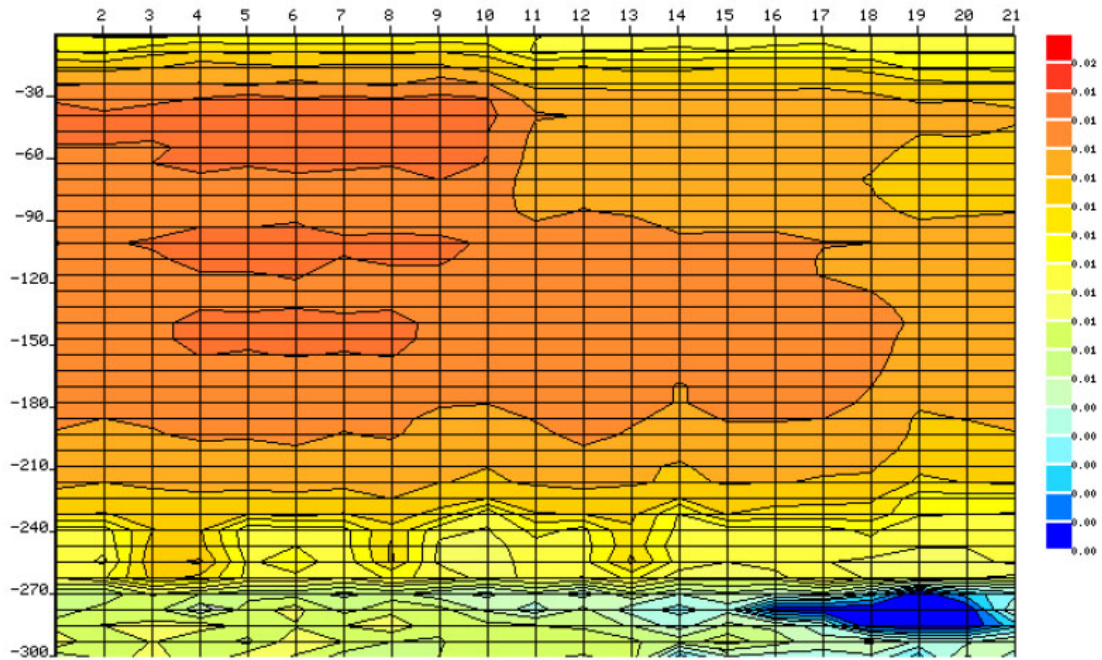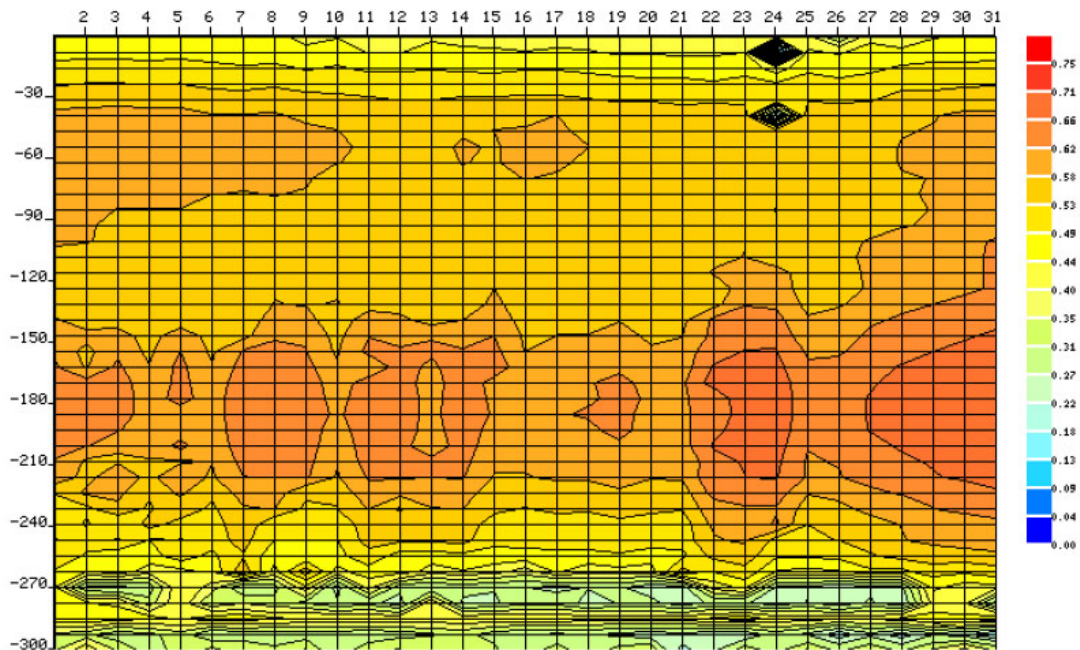

Fig. (17). Line 71 Maumbi Minahasa Utara.

Fig. (18). Line 72 Ring Road – 2 Manado city.

Line 72 Maumbi, Minahasa Utara, at the coordinate 1°29'8.86"N, 124°53'49.57"E, showed a strong zone area with no water potential. There was no fault, as shown in Fig. (**18**).

Line 73 Ring Road – 3, Manado City, at the coordinate 1°28'59.81"N, 24°53'44.98"E showed a strong zone area with no water potential. There was no fault, as shown in Fig. (**19**).
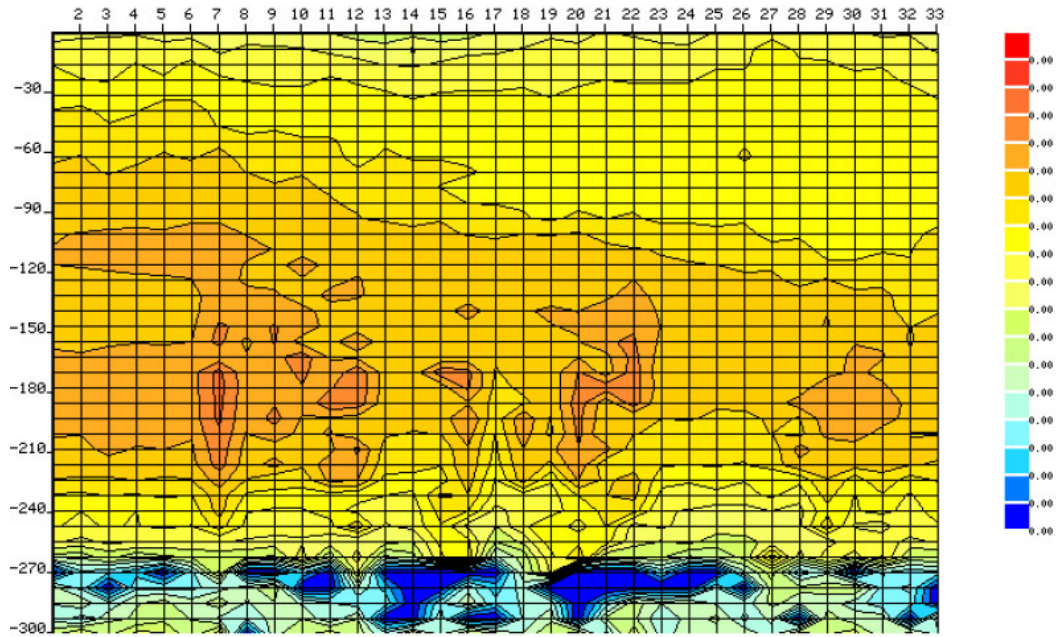

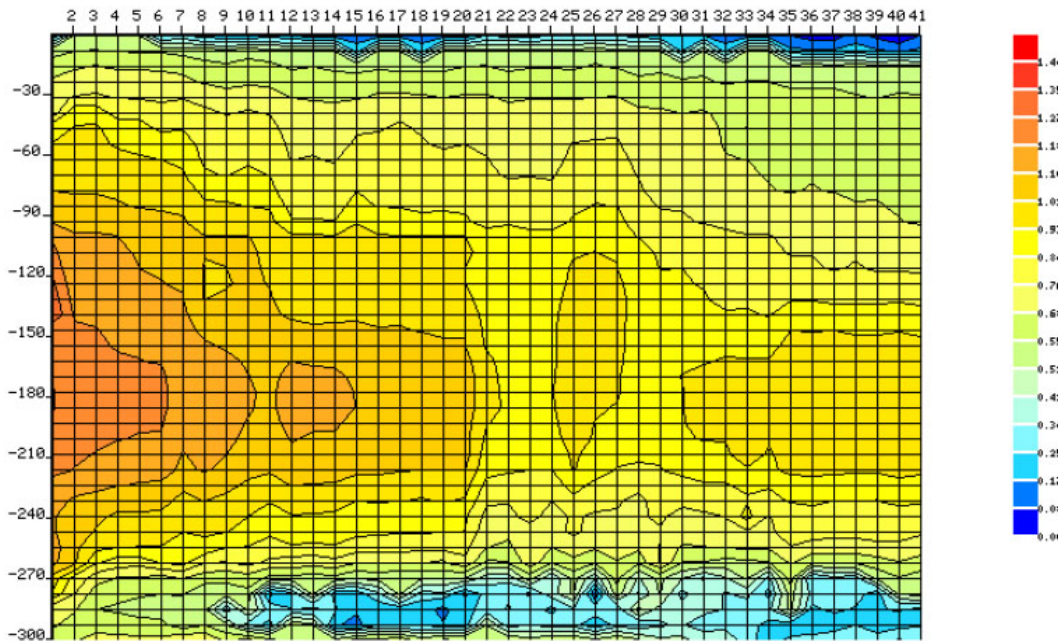
Fig. (19). Line 73 Ring Road – 3 Manado city.

Fig. (20). Line 74 Singkil Manado city.

Line 74 Singkil, Manado City, at the coordinates 1°29'18.98"N, 124°51'13.86"E, showed a strong zone area with no water potential. There was no fault, as shown in Fig. (**20**).

Line 75 Sindulang, Manado City, at the coordinates 1°29'51.91"N, 124°50'47.16"E, showed a strong zone area with no water potential. There was no fault, as shown in Fig. (**21**).

Fig. (21). Line 75 Sindulang Manado city.

Fig. (22). Line 76 Sario Manado city.

Line 76 Sario, Manado City, at the coordinates 1°28'14.57"N, 124°50'7.91"E, showed a strong zone area with no water potential. There was no fault, as shown in Fig. (**22**).
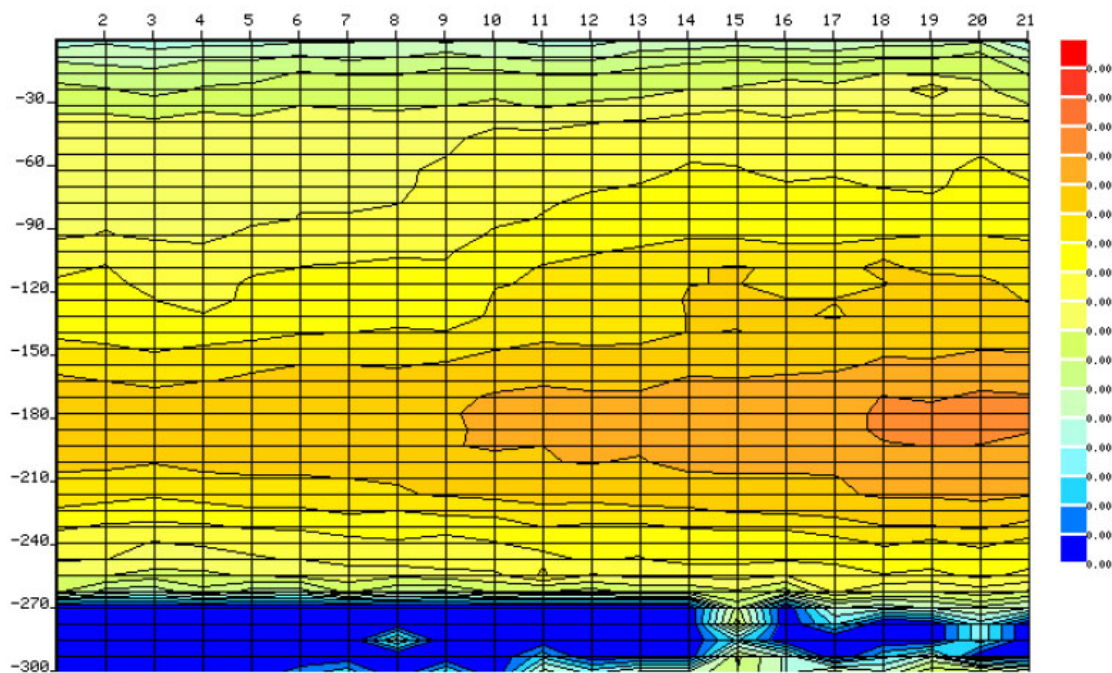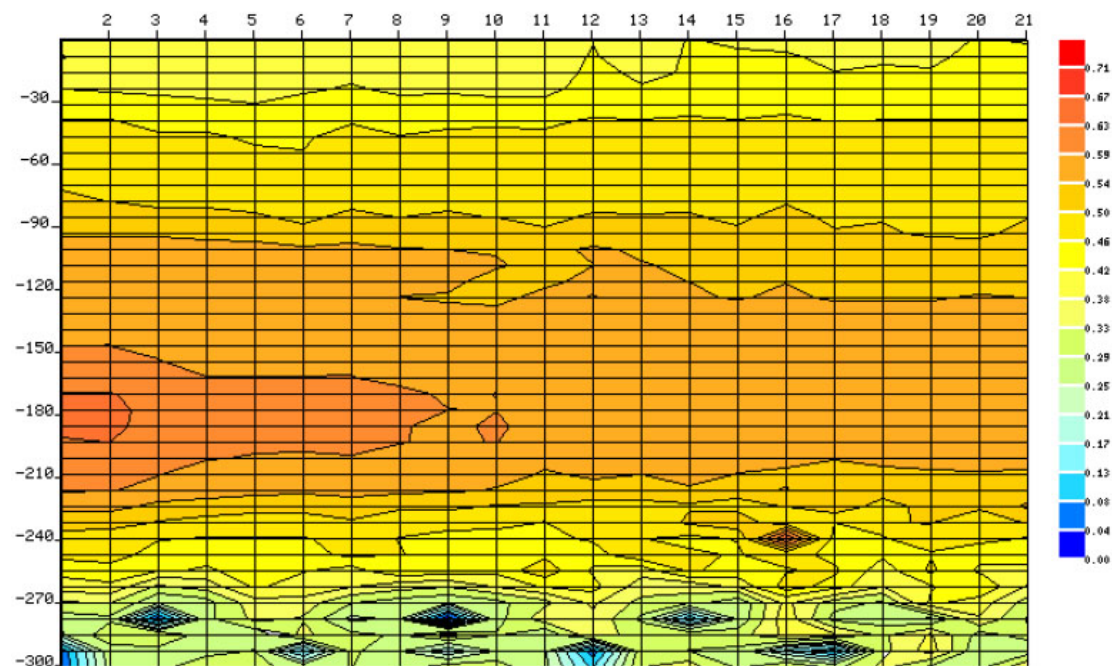
Line 77 Ranotana, Manado City, at the coordinate1°27'31.23"N, 124°50'5.32"E, showed a strong zone area with no water potential. There was no fault, as shown in Fig. (**23**).

The identification of the Manado Fault line resulted in 17 identified lines spread across Manado City. Among these 17 lines, only two lines, line 23 (Kayuragi-1) and line 70 (Ring Road, Manado City), showed faults starting from 30m to 270m, with resistivity values of 0 Ω. The Manado fault line was drawn from line 23 to line 70, as shown in Fig. (**24**).
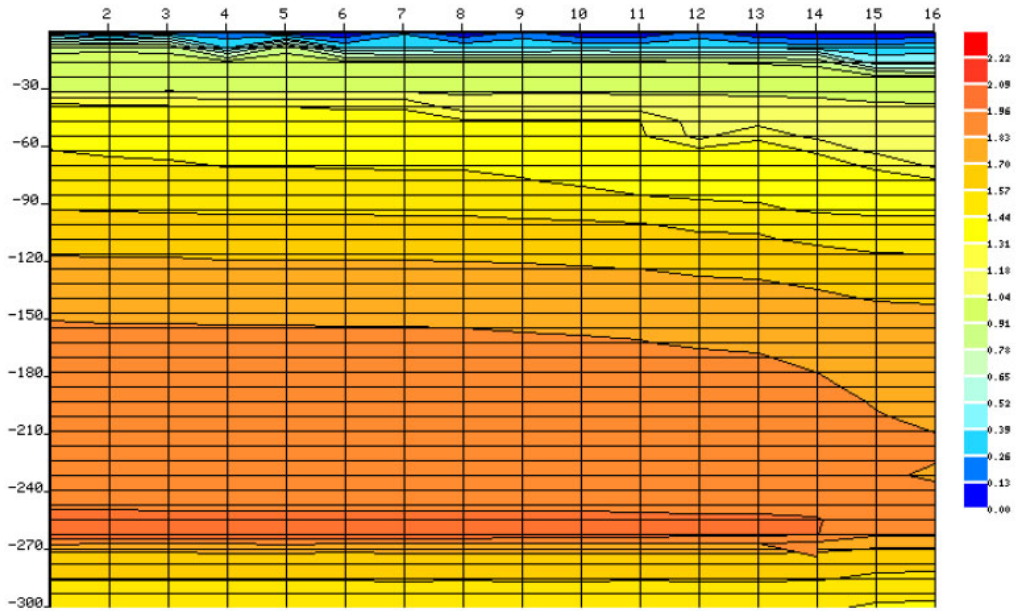

Fig. (23). Line 77 Ranotana Manado city.

Fig. (24). Result of manado fault line.

The present identified Manado fault lines were close to the previous geology map of the Manado fault line. The Manado fault line was not active from 1800 to 2023 (USGS Website). As shown in Fig. (**1**), there have been following inshore earthquakes: M 5.3 - 14 km NNW of Laikit, Laikit II (Dimembe), Indonesia Time 1980-02-22 03:51:45 (UTC) Location 1.611°N 124.929°E Depth 26.0 km; M 5.3 - 28 km N of Laikit, Laikit II (Dimembe), Indonesia Time 1984-05-31 08:43:50 (UTC) Location 1.749°N 124.961°E Depth 233.5 km; M 5.0 - 21 km NNE of Laikit, Laikit II (Dimembe), Indonesia Time 1988-08-01 04:39:57 (UTC) Location 1.663°N 125.067°E Depth 222.4 km; M 5.2 - 10 km NW of Manado, Indonesia Time 1988-08-17 23:09:40 (UTC) Location 1.555°N 124.785°E Depth 33.0 km; M 5.2 - 15 km NE of Laikit, Laikit II (Dimembe), Indonesia Time 2006-06-05 18:56:32 (UTC) Location 1.594°N 125.063°E Depth 172.9 km; M 5.2 - 11 km E of Tondano, Indonesia Time 2015-10-02 15:51:53 (UTC) Location 1.315°N 125.014°E Depth 109.8 km; M 5.2 - 37 km E of Laikit, Laikit II (Dimembe), Indonesia Time 2018-10-13 04:34:14 (UTC) Location 1.515°N 125.309°E Depth 97.2 km.

CONCLUSION

The map of the Manado fault line was found at line 23 Kayuragi -1, line 70 Ring Road – 1 Manado City, by using the PQWT T300 instrument. The Manado fault was found at 30m to 270m with a resistivity of 0 Ω. The present study of the Manado fault line was close to the previous analysis. However, the activity of the Manado fault line has not been detected since the 1800s. Still, the present method yielded a better result for the Manado fault line than the previous method.

RECOMMENDATION

Although the methods of analysis are reasonably supported by the present model tests, further line tests may be needed to support the present fault line.

AUTHORS' CONTRIBUTION

It is hereby acknowledged that all authors have accepted responsibility for the manuscript's content and consented to its submission. They have meticulously reviewed all results and unanimously approved the final version of the manuscript.

CONSENT FOR PUBLICATION

Not applicable.

AVAILABILITY OF DATA AND MATERIALS

The data and supportive information are available within the article.

FUNDING

CONFLICT OF INTEREST

The authors declare no conflict of interest, financial or otherwise.

REFERENCES

[1]   A.C. Effendi, "Center for Geological Research and Development", In: *Geological map of the Manado Sheet,,* North Sulawesi, 1997.

[2]   E.E. Siahaan, S. Soemarinda, A. Fauzi, T. Silitonga, T. Azimudin, and I.B. Raharjo, "Tectonism and volcanism study in the minahasa compartment of the north arm of sulawesi related to lahendong geothermal field, indonesia", *Proceedings World Geothermal Congress 2005* Antalya, Turkey, 24-29 April 2005, pp. 1-5.

[3]   T. Beaudouin, O. Bellier, and M. Sebrier, "Present-day stress and deformation field within the Sulawesi Island area (Indonesia) : Geodynamic implications", *Bull. Soc. Geol. Fr.,* vol. 174, no. 3, pp. 305-317, 2003.
[http://dx.doi.org/10.2113/174.3.305]

[4]   A. Cipta, R. Robiana, J.D. Griffin, N. Horspool, S. Hidayati, and P.R. Cummins, "A probabilistic seismic hazard assessment for Sulawesi, Indonesia", In: *Geohazards in Indonesia: Earth Science for Disaster Risk Reduction,* vol. 441. The Geological Society of London., 2016.

[5]   Herman Darman, *Seismic Expression of North Sulawesi Subduction Zone,,* Shell International E & P: Netherlands, 2011, pp. 5-8.

[6]   T. Zheng, Q. Qiu, J. Lin, and X. Yang, "Raised potential earthquake and tsunami hazards at the North Sulawesi subduction zone after a flurry of major seismicity", *Mar. Pet. Geol.,* vol. 148, p. 106024, 2023.
[http://dx.doi.org/10.1016/j.marpetgeo.2022.106024]

[7]   C. Lu, T. Hao, N. Rawlinson, L. Zhao, Y. Xu, and L. Liu, "Introduction to the 3-D seismic observation of the North-Sulawesi subduction zone and the study of initiation mechanism", *Mar. Geol. Quat. Geol.,* vol. 39, no. 5, pp. 131-137, 2019.

[8]   E.A. Silver, R. McCaffrey, and R.B. Smith, "Collision, rotation, and the initiation of subduction in the evolution of Sulawesi, Indonesia", *J. Geophys. Res.,* vol. 88, no. B11, pp. 9407-9418, 1983.
[http://dx.doi.org/10.1029/JB088iB11p09407]

[9]   Wm. Brian, and P.G. Schulte, "Methods of fault detection with geophysical data and surface geology", *Journal Recorder VOL,* vol. 44, no. 05, 2019.

[10] B. Suski, G. Brocard, C. Authemayou, B.C. Muralles, C. Teyssier, and K. Holliger, "Localization and characterization of an active fault in an urbanized area in central Guatemala by means of geoelectrical imaging", *Tectonophysics,* vol. 480, no. 1-4, pp. 88-98, 2010.
[http://dx.doi.org/10.1016/j.tecto.2009.09.028]

[11] P. Štěpančíková, J. Dohnal, T. Pánek, M. Łój, V. Smolková, and K. Šilhán, "The application of electrical resistivity tomography and gravimetric survey as useful tools in an active tectonics study of the sudetic marginal fault (Bohemian Massif, central Europe)", *J. Appl. Geophys.,* vol. 74, no. 1, pp. 69-80, 2011.
[http://dx.doi.org/10.1016/j.jappgeo.2011.03.007]

[12] N. Pondard, and P.M. Barnes, "Structure and paleo earthquake records of active submarine faults, Cook Strait, New Zealand: Implications for fault interactions, stress loading, and seismic hazard", *J. Geophys. Res,* vol. 115, no. B12, 2010.

[13] W.J. Seaton, and T.J. Burbey, "Evaluation of two-dimensional resistivity methods in a fractured crystalline-rock terrane", *J. Appl. Geophys.,* vol. 51, no. 1, pp. 21-41, 2002.
[http://dx.doi.org/10.1016/S0926-9851(02)00212-4]

[14] Luciano Lopez, Horatio Echeveste, Mario Tessone, Marta Alperın, and Ricardo Etcheverry, "Geoelectric exploration of the purísima-rumicruz district, Jujuy Province, Argentina", *Geophys. J. Int.,* vol. 2012, no. 2, 2012.

[15] W.M. Telford, and L.P. Goldrat, *Applied Geophysics ,* 2nd ed Cambridge University Press: Cambridge, 1990.

[16] Z. Wang, X. Cai, J. Yan, J. Wang, Y. Liu, and L. Zhang, "Using the integrated geophysical methods detecting active faults: A case study in Beijing, China", *J. Appl. Geophys.,* vol. 156, pp. 82-91, 2018.

[http://dx.doi.org/10.1016/j.jappgeo.2017.01.030]

[17] B. Brent, "Using geophysics tp map bedrock faults, dikes, and surficial geology in relation to karst features in the briery branch quadrangle, rockingham county, Virginia", *15th Sinkhole Conference, NCKRI Symposium 7* January 2000, pp. 235-240.